Southern African Large Telescope

RSS UW Commissioning Activities, 2013-2

Kenneth Nordsieck
University of Wisconsin

v 1.0
23 May, 2014

Change History

Rev	Date	Description
1.0	23 May, 2014	Original

Table of Contents

1 RSS Flatfielding Technique Development

For RSS modes beyond spectroscopy of single point objects, production of reliable flatfields over the field of view has proven to be a problem. The original plan to use QTH lamp inputs from the SALT calibration system, with the pupil/ FOV illumination variation during a track simulated using the moving baffle, has been found to be insufficient, apparently because there is significant SAC vignetting outside the pupil and field stops. Current work in this area involves:

- Modeling the telescope illumination and verifying the model using RSS imaging data.

- Measuring and modeling illumination dependence of the RSS optics.

- Developing python code for the SALT pipeline to use these models to modify observed flatfield data to account for track-dependent variation

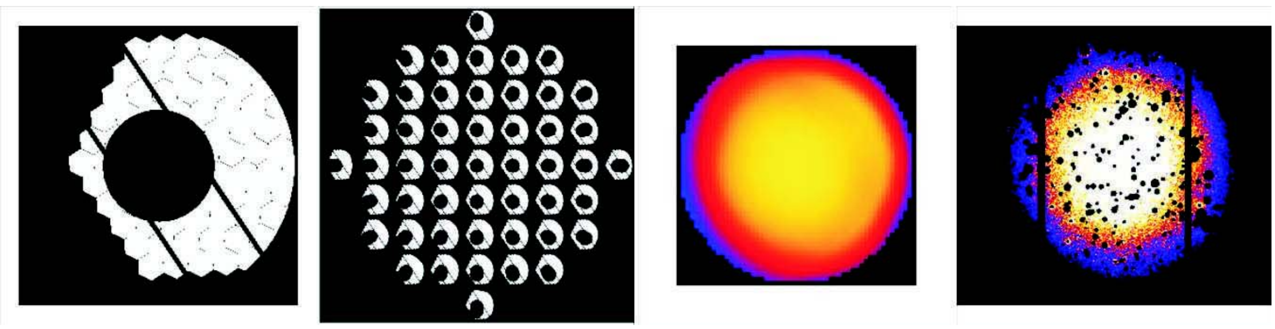

Figure 1. Start of Track

1.1 Telescope Illumination Model

The telescope illumination was modeled using the ZEMAX SAC model with the latest baffling (D. O'Donoghue, Board #32). The important feature of this model is that the SAC vignetting is a function of field angle. The vignetting boundaries at the pupil were modeled as overlapping ellipses, whose parameters vary linearly with field angle. The telescope primary was modeled as 91 hexagons, shadowed by a model of the tracker and the tracker Y-beams. The SAC input pupil was then the mirror included inside an 11m circle representing the SAC entrance pupil maximum diameter. Figure 1 illustrates the illumination model at the beginning of the track of a test imaging sequence of an SDSS field obtained for commissioning proposal 2012-2-UW-006. On the left in figure 1 is the illumination of the SAC exit pupil at field center. The second panel shows the dependence of pupil illumination on field angle, by placing a miniature pupil at each of 49 field positions in a field grid. The fact that all are not the same illustrates the field-dependent vignetting. The third panel shows the imaging flatfield for the track position, which is basically the sum of the number of rays in the pupil at each field position. Finally, on the far right is a panel showing an actual estimate of the flat field for that observation, by removing the stars from the image.

Ultimately, a flatfield correction as a function of track will be computed by interpolating in a grid of flatfields in track space. Figure 2 shows such a grid. Significant results from this exercise include:

- Toward the edge of the track area, flatfields develop a "crease" (a discontinuity in slope) caused by the intersection of the mirror edge and the SAC central obscuration.

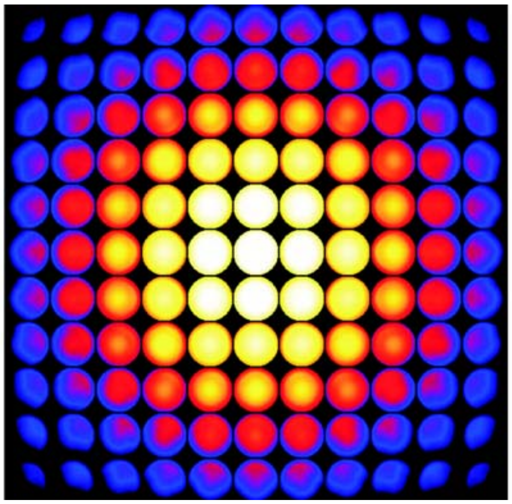

Figure 2. Flatfield in Track Space

- The flat field is relatively constant over the center 2/3 of track space, then changes rapidly at the edge. It may be advantageous to build in a narrower visibility range for programs that are flatfield-sensitive.

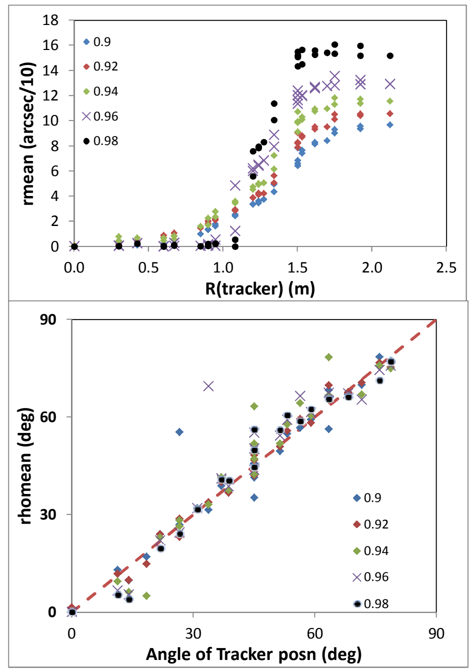

Figure 3. Flatfield contours vs track position

- The flat field does not necessarily peak on-axis. For observations far North and far South where one never comes close to track center, it may pay to observe off-axis. The change in flatfield peak with distance from center of track is quantified in Figure 3, top. For each flatfield, contours are drawn at the 90%, 92% ... 98% levels, and the distance of the center of the contour is plotted as a function of tracker distance from center. Starting about 1 m from center, the centers move systematically, with the center contours moving quite dramatically by several arcmin at 1 m out. So even the center of the flat moves systematically, which is important considering in longslit spectroscopy of centered objects, sky is often taken an arcmin from the star.

- There is substantial symmetry which can be taken advantage of: the flat shape is exactly symmetric about the tracker X and Y axes, so only one quadrant of figure 2 is unique. There is approximate reflection symmetry at other track angles, which is illustrated in the bottom plot of Figure 3, where the direction of motion of the flat center is plotted vs. the angle in track space.

1.2 RSS Optics Pupil Dependence

Once a model of the SALT illumination of the RSS field of view in imaging mode is

Mode	Model Input Required	Source	Mask	How
Fabry Perot	Etalon Vignetting	QTH Lamp	Pinhole Grid	Etalon in/ Etalon out
Grating Spectral Imaging	Grating Efficiency over FOV, uniformity	Mono-chromator	Pinhole Grid	Grating In/Out; 0-order, 1st order at various tilts
Polarimetric Imaging	Pol Vignetting, beamsplitter uniformity	QTH Lamp	Pinhole Grid + Pol mask	Beamsplitter, waveplates In/Out
Grating Spectropolarimetry	Grating Polarization over FOV	Mono-chromator	Pinhole Grid + Pol mask	Grating In/Out; 0-order, 1st order at various tilts

Table 1. Data required to calculate RSS flatfields

developed, we will need a model of the field- and pupil-dependent response of the RSS collimated area optics, to enable computation of the track dependence of the flatfield in the more complex modes. Table 1 above lists data that will be required to develop these models. This will use a pupil map observed by inserting a metal shimstock slitmask with an array of pinholes (Figure 4), and observing it with the spectrograph defocused by inserting an empty filter holder. When illuminated, an image of the pupil is produced for each point in the FOV, similar to the second panel in Figure 1. Figure 5 shows an image of the QTH lamp obtained in this manner (the light leak on the left has since been corrected). The response of the optic is then deduced by ratioing pinhole mask images taken with the optic in and out. One commissioning proposal, 2013-1-UW-006, has collected data to start testing the 3000 l/mm grating efficiency in this way,

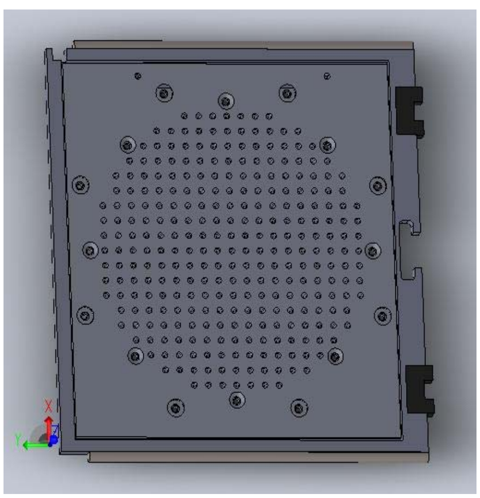

Figure 4 Pinhole Grid Slitmask

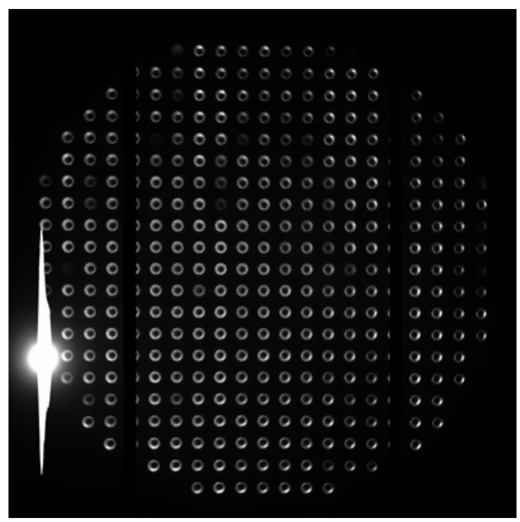

Figure 5. QTH Pupil Map Image

to calculate spectral flatfields for actual longslit data from science tracks.

1.3 Pipeline Software

To support application of flats in the pipeline, a number of python routines are being developed. The first, now complete, is an image distortion remover ("scrunch") which preserves flux. This uses a map of the location of the raw data bin corners in user space (a "bin map"). Ultimately, it will be desirable to maintain such a map as data reduction proceeds to calibrate the optic distortion, the grating dispersion, the polarimetric beamsplitter distortion, etc. The concept is to leave the actual resampling of the "scrunch" process to the very end, since each such resample loses information in resolution and introduces noise. Such a pipeline script is being developed which would maintain, as far as possible, the current calibration tools while introducing the bin map as a data product.

2 Mode Rework

2.1 Polarimetry

RSS polarimetric modes are not currently available because a coupling fluid leak developed in the polarizing beamsplitter after a year of operation. Because this was a recurrence of this problem, it was decided to redesign the beamsplitter to use a different couplant. This is complicated by the unusual thermal expansion properties of the calcite optic, and by the necessity of aligning the individual elements in the beamsplitter mosaic (RSS is the first to use a mosaic beamsplitter). Laboratory work to characterize different candidate couplants has been completed. Dow-Corning Q2-3067 optical grease has been eliminated: it appears to degrade with time. Lux-Link gel has the useful property that it does not "set," simplifying the alignment step, but the long-term stability of this couplant is in question, and it has not been used by astronomers. We have settled on Nye 451, which has been used by astronomers, including on calcite. Testing is complete on a "sacrificial" calcite prism with the same geometry as an actual mosaic element. A successful assembly has been performed, with bubbles removed and the gel set. The material is then of the consistency of "soft rubber," and an FEA model of the joint verifies that it is safe over the thermal survival range and for post-setting alignment. An extended thermal test including a large temperature swing (Figure 6) has been completed successfully (Figure 7).

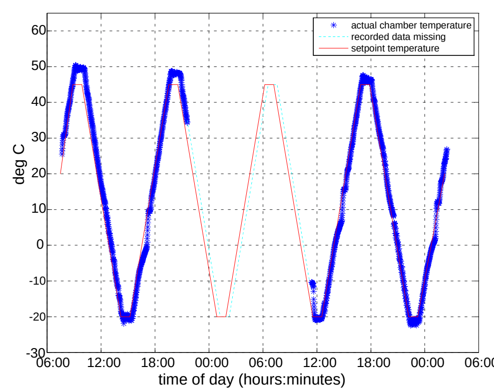

Figure 6. Test Prism Thermal Test

Figure 7. Thermal Test Survival

Assembly is proceeding: Following disassembly of the mosaic, it was found that the calcite surfaces in contact with the fluid had developed a "haze," and this has been polished off by the manufacturer Karl Lambrecht Corp. Unfortunately, one of the wedges was broken in the process, and a replacement was fabricated, glued together from three smaller wedges of available UV calcite, and AR coated by OptoSigma Corp., the original coating vendor. The wedges have been repositioned on the mosaic to put defects in the corner, beneath the pupil mask, and the replacement wedge at the center, behind the telescope obscuration. Completion is estimated in 1-2 months.

2.2 Fabry-Perot Dual-Etalon Mode

RSS dual-etalon Fabry-Perot spectroscopy is not currently available because of the discovery of severe ghosting between the two etalons in this mode. A design for modification of the etalon holders such that the etalon surfaces can be precisely aligned, and flexure is much reduced, is now complete (Figure 8). The goal is to implement this upgrade when RSS is off-telescope for upgrade of the collimator triplet optics.

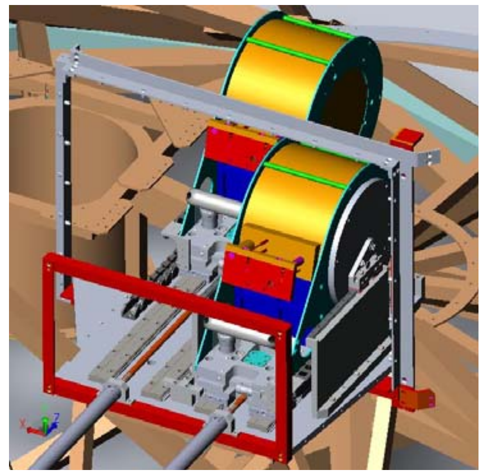

Figure 8. Etalon alignment design